

Structural Analysis of Wheels Through Analytical and Experimental Methods

Pinar Demircioglu¹, Ismail Bogrekci², Mehmet Kose³

^{1,2}Faculty of Engineering, Department of Mechanical Engineering, Aydin Adnan Menderes University, Aydin, Turkey

³Graduate School of Natural and Applied Sciences, Department of Mechanical Engineering, Aydin Adnan Menderes University, Aydin/Turkey & Jantsa Wheel Industry, Design Center, Aydin/Turkey

Abstract

Analytical and experimental methods have a complementary relationship. Finite element analysis is a key method to decrease cost and make quicker decisions. A certain degree of correlation must exist between them. In the study, analytical and experimental studies were conducted based on a new wheel size that is 8.25x20. The rim part of the wheel was designed with three different configurations which material thicknesses of 5 mm, 5.5 mm and 6 mm. Flow of the experiments was started with considering 5 mm and 6 mm in the first place. According to results taken from analyses and experiments, an optimization configuration was designed as 5.5 mm. Radial fatigue test was chosen as physical test and analysis setup was built on it. Since the results of finite element analysis were used in fatigue life calculations, it was validated with mesh independence less than 1% variation by assignment of boundary conditions and loadings calculated from the authoritative literature. The importance of the optimization process to keep a product competitive in the market was shown by weight reduction. Fatigue life cycle correlation was performed in the first case resulted with 7.35% difference between physical radial fatigue test and finite element analysis. The analyses and fatigue calculations indicated extremely high cycle counts make the physical tests impractical and not feasible to align the test cycles with the calculations in the other cases. Therefore, the physical radial tests for the other cases were finalized at a point meet with the cycles well above the test standard limits, and durability of the wheels in the other cases were confirmed.

Keywords: Fatigue Life, Finite Element Analysis, Wheel, Radial Fatigue Test, Correlation, Optimization.

1. Introduction

Transportation, agriculture, and mining are built on these vehicles that have different applications and loadings. Wheels join the game as a safety part for the vehicles. Wheels should endure challenging applications and high load capacities. Therefore, design processes of wheels have to be comprehensive to be sustainable against demanding requests of the industries.

A research study in European Mechanical Science conducted a rotating bending test. A356-T6 was used as wheel material. The short- and long-term physical tests and finite element analyses were performed on the selected wheel. Zinc-glycerin was used as a crack detection tool in the test. In the short-term physical test, the experiment concluded at 2.5 million cycles, with crack initiation observed at around 225,000 cycles. Additionally, 10 million cycles were completed in the long-term physical tests. Convincing results were obtained from the analysis, S-N curve, and physical tests [1].

A study focused on improving the wheel made of aluminum. Two models were performed on the rotary fatigue test and analysis. 5 nodes on the wheel body were selected from base and improved designs. In the end, improved design was convincing, but the base model wasn't. Simulation results and physical test results were confirmed by each other [2].

There was a study done with specific emphasis on carrying out FEA of a particular steel wheel with varied applications of radial loads. In this study, there was an application of the distributed radial load at multiple angles to comprehensively understand its impacts. Results of the study revealed that at an application of a radial load at an angle of 120 degrees, such a configuration delivered results most like those of physical test results. On the other hand, other tested angles such as 60 degrees as well as 90 degrees delivered levels of results significantly differing as well as less in alignment with physical test results [3].

A study conducted on a multipiece steel wheel of size 25-19.5/2.5 demonstrates an improvement in material quality. The study focused on the gutter side of the wheel, highlighting areas of failure. A remarkable performance increment was given by changing the material quality from S355 to S690 [4].

Impact test correlation was conducted in a SAE paper. 4 strain gauges were used in physical tests to compare max. and min. principal strains taken from analysis. -1% and 3% of deviations were observed while 0% was observed in min. principal strains [5].

Another physical wheel test named radial fatigue test was conducted in a SAE paper for correlation. When the strain gauge results and finite element analysis results were compared, closest results were obtained in max. principal stress between von-misses, min. principal and max. principal stresses [6].

Different wheel materials were taken into consideration for the optimization process. Steel stood out among the selected materials in the study which are steel, carbon fiber, aluminum alloy, magnesium alloy and titanium alloy [7].

Another similar study performed different materials present that steel alloy have a higher cycles than forged steel, aluminum and magnesium wheels [8].

Correlation between experimental and analytical results were studied. The study had some deviations because of the optimum element size, but it was still confirmed since the results have similar patterns [9].

A study from literature presented durability, fuel consumption, mass and emission factors in material selection. The study emphasized the current expectation in the industry. Steel was determined as more durable while aluminum was better from other sides [10].

Existing literature and industry demand clearly shows the requirement of correlation and optimization in wheel design. The aim of the study is clarifying new product development with the correlation stages from extensive physical fatigue testing and finite element analyses strengthened by optimization and radial loading approach.

2. Material and Method

In the study, 3 different material qualities were used. Disc material quality was S355 for all three cases. Disc thickness was 10.5 mm, and production method was flow forming. Optimization process is performed at the rim part of the wheel. Material qualities were S275 for rims with thickness of 5 mm and 5.5 mm and S420 for rim with thickness of 6 mm. All three materials compiled with the defined specification range. Material quality has a direct effect on fatigue life. That's why material selection has a critical role in manufacturing suitable products in the industry. Also, evaluation of product purchasing is another important criterion during the selection process. Comprehensive investigation in market illuminates the whether the process can be continuous or not in future for purchasing.

Pre-design processes of the material were performed on SolidWorks software. Figure 1 shows the 3-dimensional visual of the specified wheel model from isometric and top views. The rim size was 8.25x20 and different material qualities and thicknesses were considered for the rim part. The thickness and material quality of the disc part kept equivalents for all of the cases. It was flow formed from 11 mm structural steel according to a specific hub. It was turned from 11 mm to 10.5 mm in the hub area. 10 bolt holes and 5 ventilation holes were used in the design for this application. Ventilation holes play a role in cooling processes of sub-components of the vehicle.

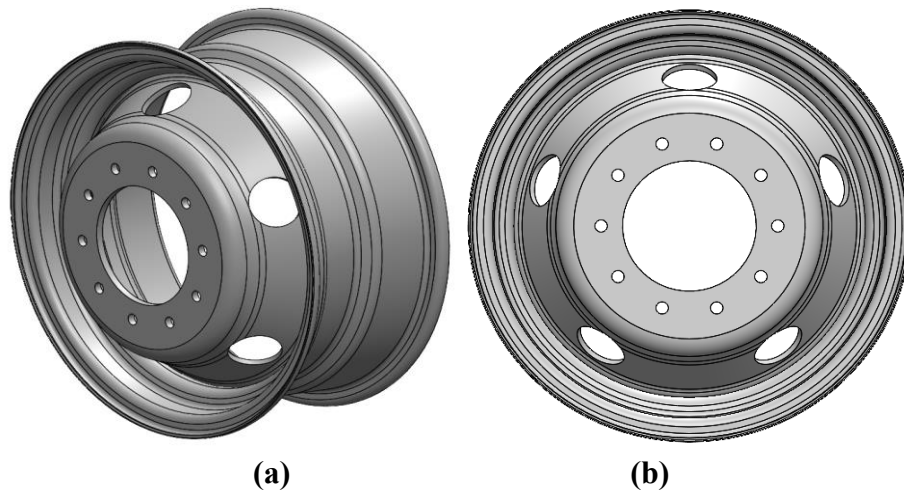


Figure 1: 3-dimensional views of wheel: (a) Isometric view, (b) Top view

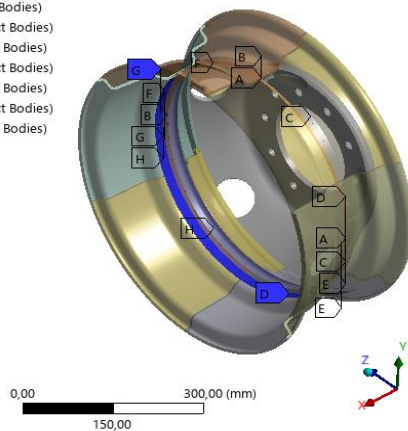
Finite element analyses have been carried out with extreme care using the sophisticated and powerful capabilities provided in the software package of ANSYS Mechanical. It begins with a considered set of assumptions especially designed for this wheel model in such a way that non-essential things, which would not contribute significantly towards final results, have been intentionally neglected. This specific step not only allows simplified analysis but also allows considerable time saving, which is of immense good use in further stages of this complete process. After this first step was carried out, a detailed identification of all faces as well as bodies relevant in this context was carried out, as this is a required base sign in this next step of procedures in progress. In some of those latter stages of this analysis, especially in those final concluding stages, there is an orderly application of boundary conditions along with the application of loads in those identified faces, with the motive of correctly modeling this whole analysis. As this setup procedure got underway to allow this complete analysis, this very first step allowed selection of material properties in this software module. Subsequently, with a clear-cut focus on connectivity of this rim, this disc, as well as this weld component, a distinct identification was created, as seen in Table 1. Also, in Figure 2, there is a pictorial view of contacts as defined in this software platform, as it is instrumental in allowing this analysis to move with ease.

Table 1: Connections between parts in the finite element analysis

Connected Parts	Connection Type
Rim and Disc	Frictional
Weld and Rim	Bonded
Weld and Disc	Bonded

Bonded - Weld2 To Rim4

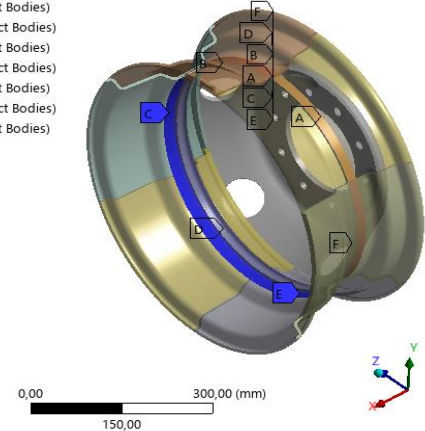
- A Bonded - Disc To Weld1 (Contact Bodies)
- A Bonded - Disc To Weld1 (Target Bodies)
- B Bonded - Disc To Weld2 (Contact Bodies)
- B Bonded - Disc To Weld2 (Target Bodies)
- C Bonded - Weld1 To Rim1 (Contact Bodies)
- C Bonded - Weld1 To Rim1 (Target Bodies)
- D Bonded - Weld1 To Rim3 (Contact Bodies)
- D Bonded - Weld1 To Rim3 (Target Bodies)
- E Bonded - Weld1 To Rim1 (Contact Bodies)
- E Bonded - Weld1 To Rim1 (Target Bodies)



(a)

Frictional - Disc To Rim1

- A Frictional - Disc To Rim1 (Contact Bodies)
- A Frictional - Disc To Rim1 (Target Bodies)
- B Frictional - Disc To Rim6 (Contact Bodies)
- B Frictional - Disc To Rim6 (Target Bodies)
- C Frictional - Disc To Rim5 (Contact Bodies)
- C Frictional - Disc To Rim5 (Target Bodies)
- D Frictional - Disc To Rim4 (Contact Bodies)
- D Frictional - Disc To Rim4 (Target Bodies)
- E Frictional - Disc To Rim3 (Contact Bodies)
- E Frictional - Disc To Rim3 (Target Bodies)



(b)

Figure 2: Contact Definitions: (a) Bonded contacts, (b) Frictional contacts

Meshing process is required in a complete and detailed manner such that it includes both the sensitivity in the obtained results as well as the time it takes to obtain those results efficiently. It is with this in view that the major methodology used in meshing is evident and presented in table 2. It is worth mentioning that due to being considered as an adequate option to apply when dealing with rim part of the model, it is of vital importance to mention the fact that using edge sizing is of valuable benefits. It is especially valuable in optimizing crucial portions of the mesh as well as in minimizing the number of elements in general being used to analyze them. For example, the rim location of critical stress area has been particularly optimized using edge sizing to obtain more sensitive results along the stated pathway in this research work.

Table 2: Mesh methods in wheel parts

Parts	Connection Type
Rim	Edge Sizing
Disc	Patch Conforming Method (Tetrahedrons)
Weld	Patch Conforming Method (Tetrahedrons)

Additional optimizations on mesh structure of disc part and weld part were performed by using edge sizing and face meshing (not for the weld part) methods. These optimization procedures serve a vital function in drastically decreasing required computations time in order to solve necessary computations, all while retaining results in sensitive regions in inviolation. Moreover, result sensitivity in extremely crucial regions such as both the mounting faces of both the hub as well as in those of the nuts was improved using these specialized tools as well as procedures. In Figure 3, one is clearly presented with an illustration showing how this mesh structure of several wheel parts is presented, including in this case, the rim in section (a), the disc in section (b), as well as this weld in section (c). In order to promote some degree of comparability in reliance between these differing wheel models under review, element numbers had been kept on purpose at levels in order to promote comparabilities across such diverse wheel models. There existed a total of some 257,000 elements together with around 820,000 nodes in use in combination throughout those models that have been reviewed as well as considered.

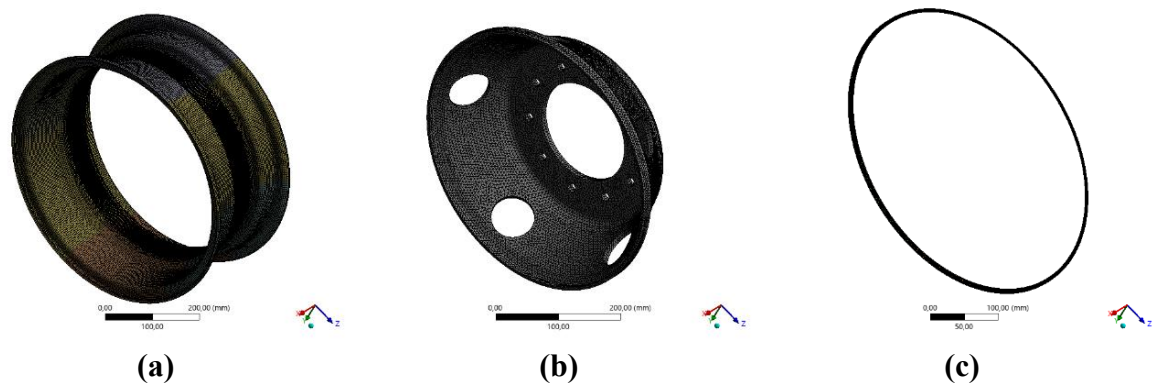


Figure 3: Mesh structure on the wheel parts: (a) Rim, (b) Disc, (c) Weld

Assembly of the wheel to the axle of the vehicle made from the defined faces in the pre-processing. Figure 4 shows defined areas for support between the wheel and hub on ANSYS. Mount faces of the nuts were defined as fixed support while hub mount face was defined as frictionless support.

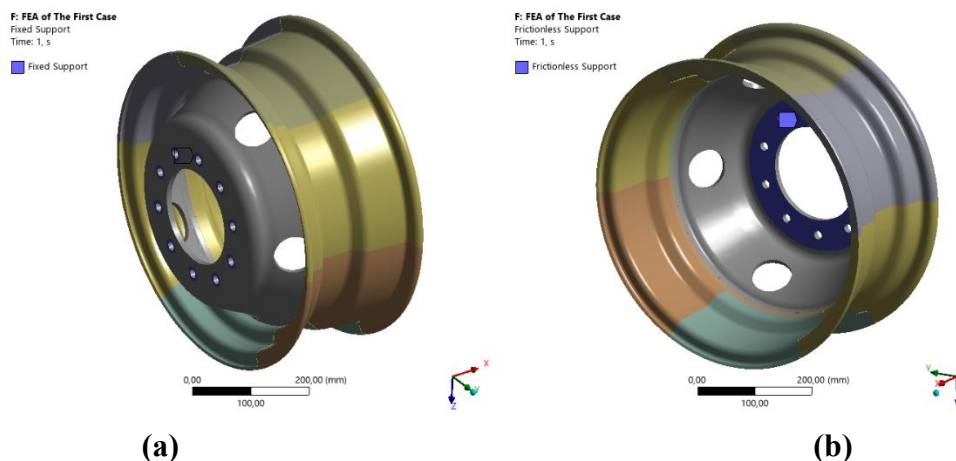


Figure 4: Wheel connection to vehicle: (a) Nut mount faces (fixed supports), (b) Hub mount face (frictionless support)

Loading conditions were decided according to load capacity of the wheel and test standard coded as EUWA ES 3.11. The standard is named Test Requirements for Steel and Aluminum Wheels [11]. Also, tire parameters were taken from the tire specifications. Table 3 shows the parameters used in the calculations of loading conditions.

Table 3: Analysis parameters [11]

Parameter	Magnitude
Loading Capacity	2270 kg
Tyre Inflation Pressure	6.5 bars
Test Acceleration Factor (EUWA ES 3.11)	2.2

The loading conditions in the analysis conducted were applied as shown in Figure 5. First, tire inflation pressure was applied taken from the tire specifications. Later, axial tire air pressure was calculated to observe axial load which transferred from tire to rim flange. Finally, bead seat radial pressure was

calculated and applied as distributed load for simulating radial pressure coming from tire. Current literature and accumulated knowledge of the company comes from numerous analyses and physical tests gave direction to the methodology. Numerous analyses were performed to reach the most possible result with 90° loading and 120° loading. According to real life results and previous literature, 120° loading was chosen for the analysis.

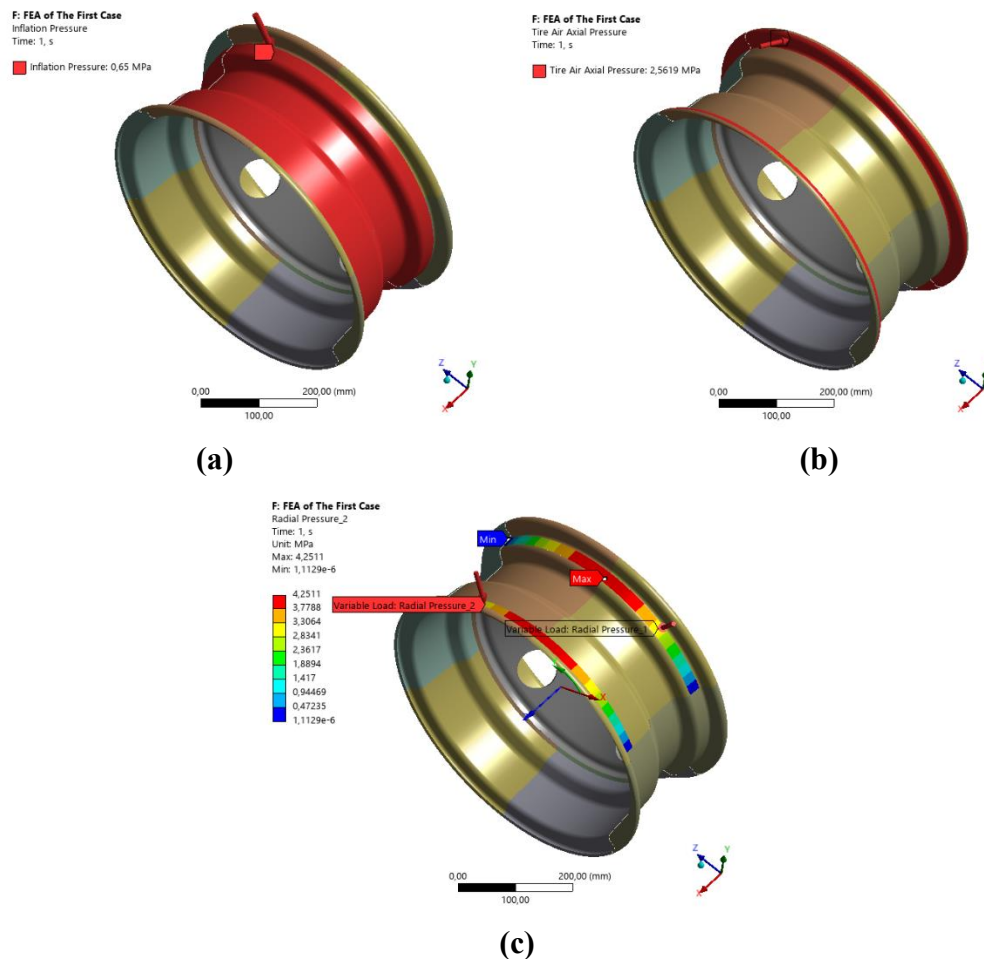


Figure 5: Loading Conditions: (a) Inflation Pressure, (b) Axial Tire Air Pressure, (c) Radial Pressure

Fatigue life calculations were based on the Gerber Theory since the materials are structural steels. Stress reduction factor plays a critical role in reaching close cycles to real life. The stress reduction factor includes marin factors named surface factor (k_a), size factor (k_b), load factor (k_c), temperature factor (k_d) and static stress concentration factor (k_e). According to these factors, the stress reduction factor was found to be around 0.39. It has very little deviation for three different material thicknesses, so the deviation was ignored.

Physical testing was performed in the radial fatigue test machine according to EUWA ES 3.11. Radial fatigue tests offer useful approach for the manufacturers to observe the wheel performance before running on the roads with the guidance of the standards. The test standard present test bench requirements, product durability requirements and formulations and coefficients for calculations to the wheel industry. Figure 6 shows a picture of the wheel subjected to this study on the radial fatigue test bench. Requested cycle by

the test standard was 500,000 cycles with 2.2 acceleration factor in physical radial fatigue tests [11]. The assembly welding of the rim and disc parts was inspected using macro analysis during production. The wheels were periodically inspected and tested at the end using the non-destructive liquid penetrant technique.



Figure 6: The wheel on the radial fatigue test bench

3. Results and Discussion

ANSYS Mechanical software was used to observe max. and min. stress results that were used in the fatigue life calculations. Maximum principal stress distributions were used in the evaluation process because of better presentation of crack occurrence. Therefore, maximum principal stress gives more sensitive results on critical fatigue crack areas.

For the reliability of the finite element analysis results and validating analysis model a mesh independence study was performed. Figure 7 shows the results vs. mesh numbers. As seen from the graph, inconsistent results were taken from the software till reaching 182,200 elements in the mesh. Since the results are mesh dependent before that number, inconsistent and wrong results were obtained. The analytical model couldn't calculate stress distribution because of less number elements than required. It causes to skip critical areas such as radiuses and contacts. An analysis model could be counted as reliable with mesh independence and proper boundary conditions. In this study, mesh independence investigation was concluded with a variance of less than 1%, and all analyses are conducted independent from mesh.

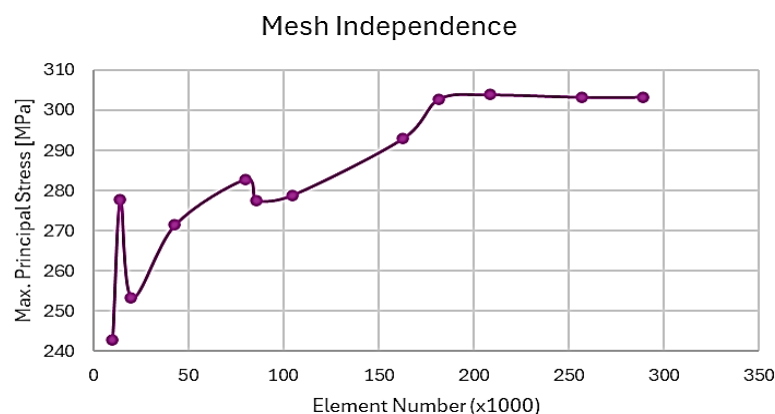


Figure 7: Mesh independence graph

The equivalent flow formed disc was used for all cases. Its material quality was S355. Figure 8 shows the first case results at once. After numerous analyses to reach mesh independence, these results were counted as reliable. As mentioned, the disc was equivalent. The rim part had a 5 mm material thickness while its material quality was S275. On the left side of Figure 8, maximum principal stress distribution is shown. As seen, the critical region was the base radius of the rim, and the maximum principal stress value was found to be 303.28 MPa. After detecting critical region for the rim, a path was created to examine and take input for fatigue calculation. This created path is shown on the right side. Mesh structure on this path was improved. From that part min. principal stress value on the critical region was obtained as 154.70 MPa.

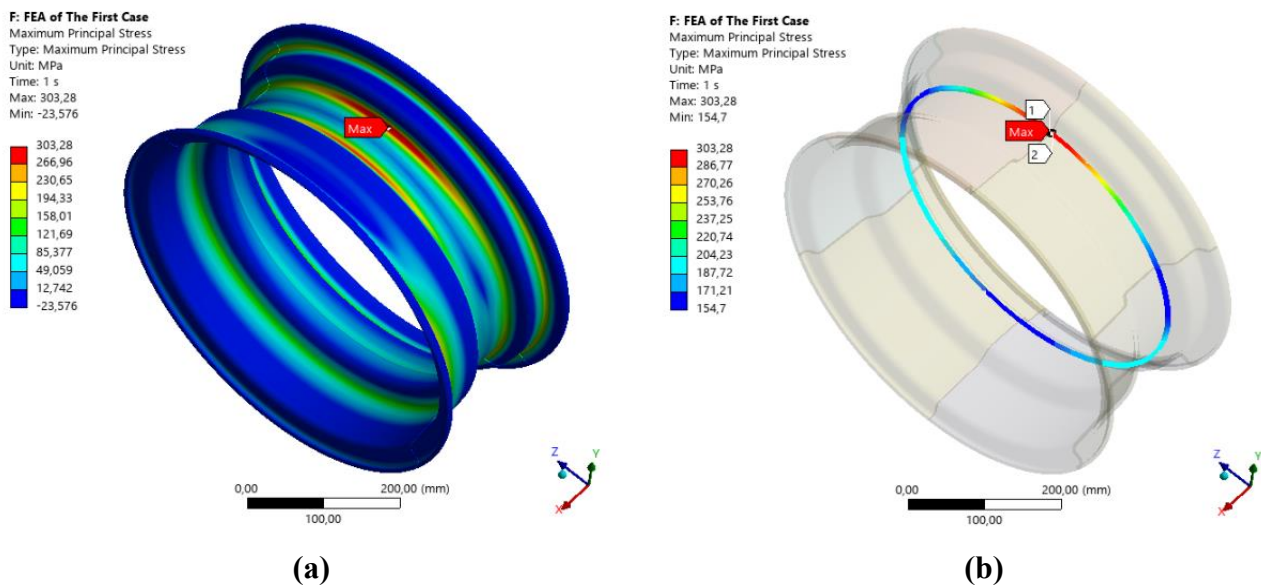


Figure 8: Maximum principal results (1st Case): (a) Rim, (b) Path

The min. and max. principal results for the first case were taken to calculate mean stress and stress amplitude in the fatigue life calculation. Table 4 listed the results during fatigue calculations according to Gerber theory. According to results in Table 4, the following S-N graph was drawn as presented in Figure 9. The calculated fatigue life cycle was obtained as 356,416 cycles. The physical radial fatigue tests failed around 332,000 cycles. Results of experimental and analytical results with a very close deviation of 7.35% show that this option for the wheel was insufficient.

Table 4: Fatigue life calculation results for the first case

Result Definition	Magnitude [MPa]
Stress Amplitude	74.29
Mean Stress	228.99
Endurance Limit	224.50
True Fatigue Strength	87.56
Corrected Fatigue Limit	64.78

The rim with material thickness of 6 mm and material quality of S420 was the second case for improving the strength of the rim. The results obtained from the first case had shown necessity of increasing material performance. When this design put into finite element analysis the following results presented in Figure

10 received from the software. A stress decrease was expected after material thickness and quality were increased. As expected, max. principal results were dramatically decreased. Max. principal stress distribution on the left side given a stress result of 227.09 MPa. The improvement on the rim resulted in around 33% max. stress reduction. When a path was created on the critical region of this case, min. principal stress was obtained as 125.25 MPa.

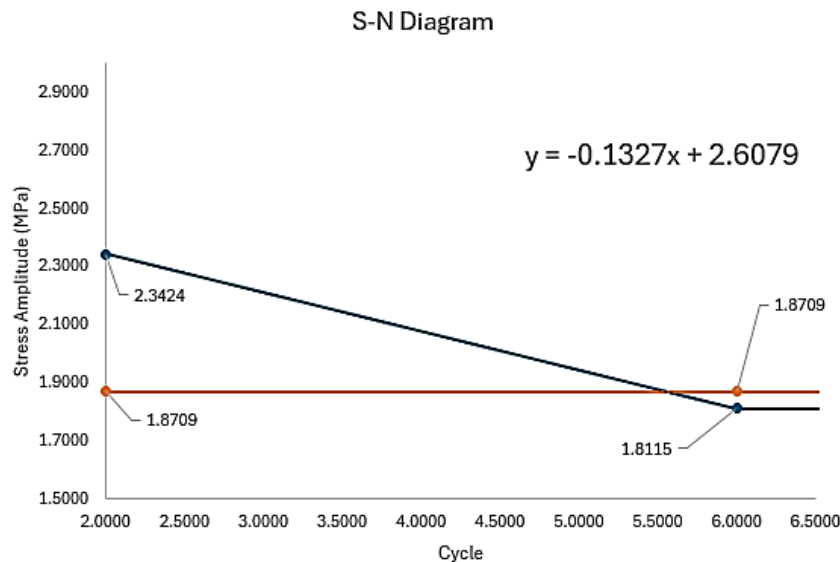


Figure 9: S-N graph of the first case

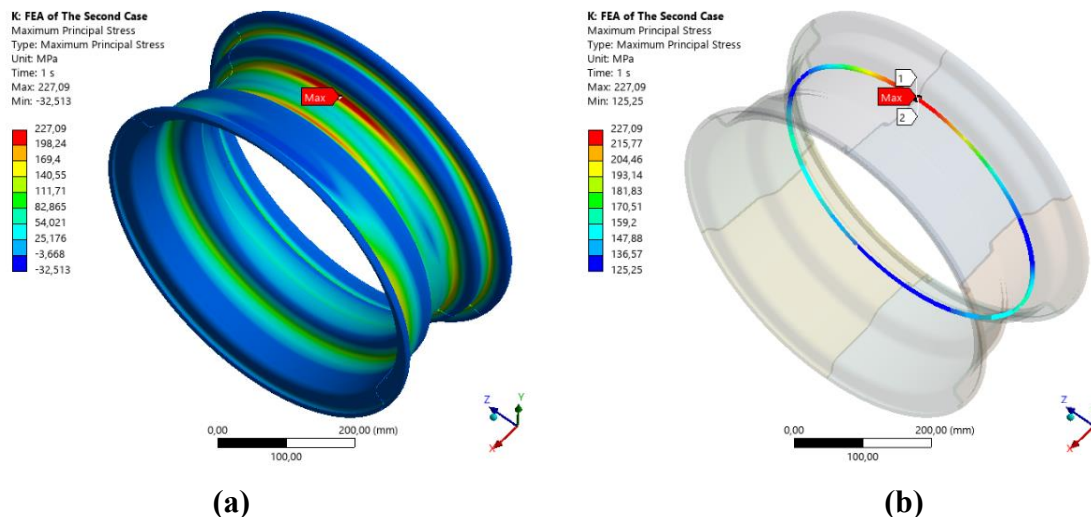


Figure 10: Maximum principal results (2nd Case): (a) Rim, (b) Path

The findings of stress amplitude as well as mean stress were seen to reduce in alignment with those acquired as a result of the detailed analysis, as expected with prior understanding. It is further interesting to know that other findings have similarly seen a reduction in the computations of fatigue as well. These findings have been presented in detail in Table 5 as required. Moreover, the finding of a substantially increased number of fatigue life cycles was evident with these results, revealing one of the essential details of the study.

Table 5: Fatigue life calculation results for the second case

Result Definition	Magnitude [MPa]
Stress Amplitude	50.92
Mean Stress	176.17
Endurance Limit	271.00
True Fatigue Strength	105.69
Corrected Fatigue Limit	94.52

The calculated fatigue life was obtained as 67,358,341. This cycle for a wheel is too high to see in a physical test, but physical radial tests were still conducted to see performance of the wheels according to second case till a point. Two physical tests were performed on the test bench and no crack or crack initiation were observed at the end of the test. One of tests was performed till 900,000 cycle. Figure 11 shows the S-N diagram of the second case.

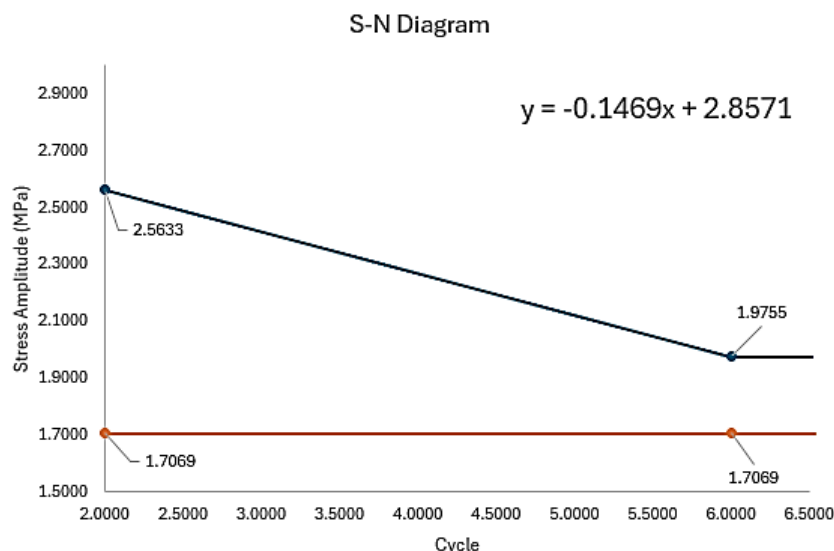


Figure 11: S-N graph of the second case

The second case gave sufficient results after physical tests and finite element analysis. However, obtained results from them gave a performance more than required. Product design is a comprehensive process that should be considered manufacturing, tooling, cost and time. Therefore, the cost of material had to be considered to avoid extra material being sustainable and competitive. It means only getting good results from the physical tests and finite element analyses are not enough to be successful, and feasible results had to be also taken. The final case also it can be named as optimization is conducted under parameters between first and second cases. The rim was designed with 5.5 mm material thickness while material quality was decreased to S275. This optimization decreases the weight of the wheel by around %8. Figure 12 shows observed max. principal distribution in optimization case. Max. stress value observed on the rim was 259.84 MPa. 139.29 MPa stress value observed as min. on the created path in the critical region. The results were expected since the maximum stress value was between the first and second cases.

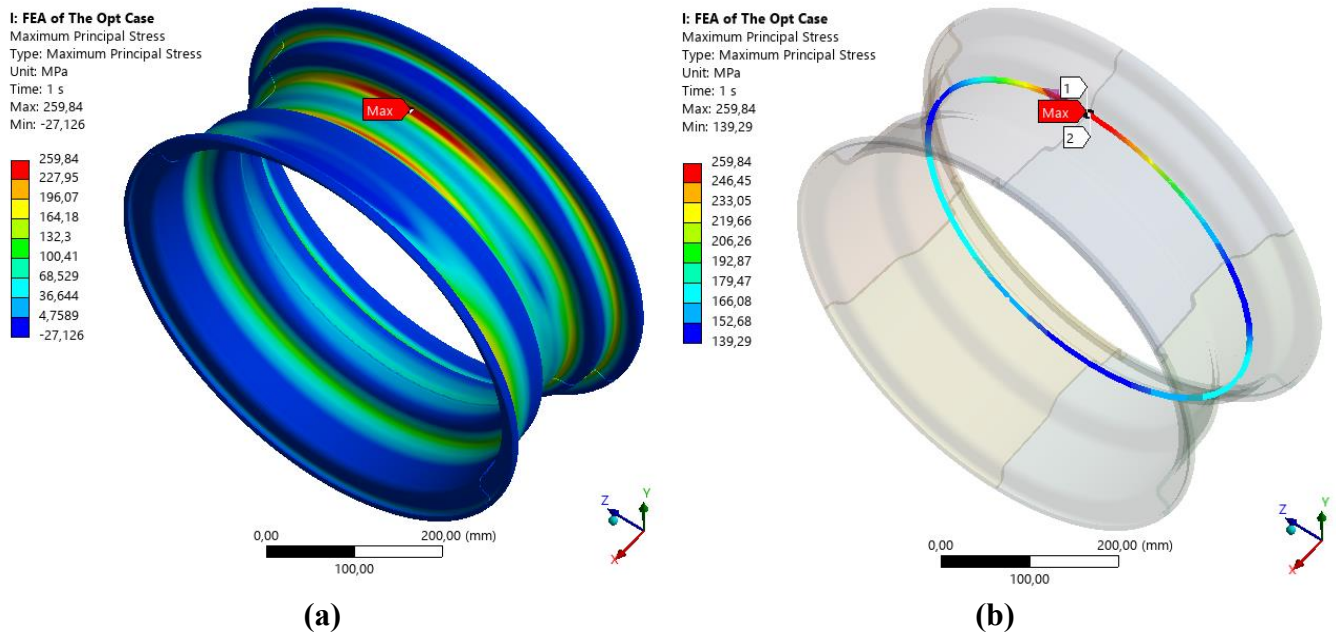


Figure 12: Maximum principal results (Optimization): (a) Rim, (b) Path

The values presented in Table 6 have been accurately determined using the application of both maximum as well as minimum results obtained in the detailed study conducted. Notably, these values always remained well within the range clearly provided by parameters set in both the first case as well as in the second case already cited in preceding elaboration.

Table 6: Fatigue life calculation results for the second case

Result Definition	Magnitude [MPa]
Stress Amplitude	60.28
Mean Stress	199.57
Endurance Limit	224.50
True Fatigue Strength	87.56
Corrected Fatigue Limit	70.26

The values determined with an extremely high degree of care and precision at the culmination of detailed computations in relation to fatigue life in this particular instance are presented in a fairly clear-cut manner in the S-N diagram shown in Figure 13. In this specific situation, a gargantuan number of 3,046,910 cycles was unearthed as a direct outcome of this particular instance of optimization under review. In conjunction with this in-depth analytical study, actual procedures of radial testing in relation to fatigue were conducted with the intention of testing, verifying, and confirming the obtained values with calculation. In a similar manner, in this second case under review, test cycles in number, matching expectations in light of computations of fatigue life, proved extremely high in nature. As such, the physical testing procedures were concluded at a definitive time, which proved ample in testing the product as being reliable as well as dependable in nature of use.

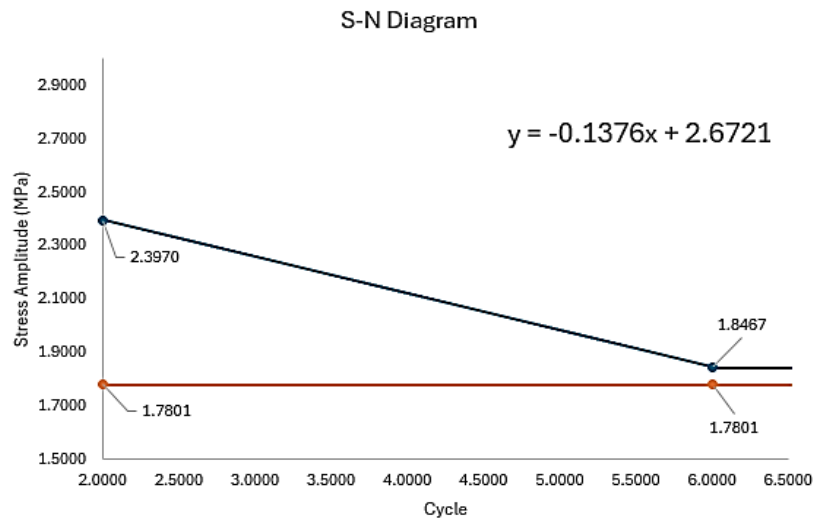


Figure 13: S-N graph of the optimization case

Three different designs were conducted in physical radial fatigue tests and finite element analyses. The overall process showed the importance of optimization by considering material waste and durability. Table 7 shows the finite element analysis results for all three cases.

Table 7: Finite element analysis results of the study

Case	Maximum Principal Stress [MPa]	Minimum Principal Stress [MPa]
1	303.28	154.70
2	227.09	125.25
3	259.84	139.29

Physical radial fatigue tests were performed on the calibrated test bench for all three cases. Two samples are taken into physical tests. The fatigue test cycles, and fatigue life calculations are listed in Table 8. Both tests were finished till reaching failure only for the first case which is designed with a rim which had a material thickness of 5 mm. Maximum principal stress on the finite element analysis was obtained on the base radius of the rim while air leakage was started from welding area of the rim. Such structures contain weld joints and transitions between different parts which have different material thicknesses and qualities should be investigated holistically. The analysis model was validated for mesh independence using the specified boundary conditions and load calculations accepted in the literature. The underlying cause of the results was the ambiguity in manufacturing processes, which may lead to microstructural defects, porosity, or residual stresses. Also, welding area couldn't be evaluated by ignoring the other areas. The weld area may be affected by the radius of the rim base. However, analytically validated results taken for fatigue calculations give very close cycles to physical radial fatigue test results which deviation is only 7.35%. Physical tests for the second case ended at a point that counted reliable. Since the expected test cycles are not feasible to finish and no crack or crack initiation were observed, it was terminated once it was deemed adequate. An increase in the fatigue life cycle and decrease in stress values were expected. The final case was designed with 5.5 mm rim. The results from the analysis took place between the first two cases as pleased. Wheels performed at the radial fatigue test benches performed the cycle limits in the specified standards well above in the second and optimization cases. The results are also highlighted that the

experimental approach and numerical analyses demonstrate a complementary relationship. Table 8 lists the results comes from physical tests and fatigue life calculations.

Table 8: Overall results and comparison

Case	Thickness	Radial Fatigue Test [Cycle]			Fatigue Life Calculation [Cycle]	Deviation [%]
		Physical Test [x1000]	Physical Test [x1000]	Ave. of Physical Test [x1000]		
1	5 mm	301	363	332	356,416	7.35
2	6 mm	900	550	725	67,358,341	-
3 (OPT)	5.5 mm	681	637	659	3,046,910	-

4. Conclusion

The importance of the correlation and optimization process was emphasized in the study. The important stages of the design were highlighted like considering material waste. It showed that designs with less material use can carry required load capacities. 3 different designs were conducted in physical radial fatigue tests and finite element analyses. All physical tests are conducted under the parameters of related standards. Before starting the finite element analyses, mesh independence of the setup was verified as mentioned in Figure 7 by evaluating stress variations. The stress variation of less than 1% shows successful refinement in the meshing process and confirms numerical stability of the analyses in the study. Firstly, the wheel design started with the lowest thickness for this study which is 5 mm. The results obtained from the tests and analyses showed that the product with these specifications was not enough to carry such loads. Although max. principal stress was observed in the base radius of the rim, air leakages were located in the weld area. This discrepancy is caused by the ideal model of welding in the analysis that couldn't represent the microstructural defects, porosity, residual stresses arising from manufacturing processes. Also, high stress area on the radius in rim could cause secondary effects to start sensitive areas in welding structure. Therefore, failures observed on the welding area are not isolated from the overall structure and affected from the rim base radius. As a result of the first case, such geometries have transitions between parts should be designed and evaluated as a whole. Secondly, material thickness was increased to 6 mm with a material quality increase. As expected, the fatigue life results showed an increase. Also, physical tests confirmed the fatigue life calculations till a point. However, weight increase caused by material thickness increment was considered as not feasible. Therefore, an optimization for a new rim was conducted. The rim material quality and thickness parameters are selected as S275 and 5.5 mm, respectively. The disc part was kept equivalents for all cases. The results obtained from analysis and physical tests were reliable enough to comment as the product was ready to carry such loads. The fatigue behavior of a steel wheel which has a new size was investigated by using analytical and experimental methods. Finite element analyses were conducted with the given boundary conditions by validating with mesh independence. Importance of the integrated assessment and physical test requirements for such products were represented. The study offers academic insight into new product development with a radial loading approach.

5. References

1. Ceylan O., & Aydoğan F., “Validation of A356T6 automobile wheel fatigue strength using the finite elements method”, European Mechanical Science, 2022 6(3), 207-212, 10.26701/ems.1117395.
2. Wang L., Chen Y., Wang C., Wang Q., “Fatigue Life Analysis of Aluminum Wheels by Simulation of Rotary Fatigue Test”, Strojnicki Vestnik, 2011, 57. 31-39. 10.5545/sv-jme.2009.046.
3. Unal C., Bogrekci I., Demircioglu P., “Modeling with Finite Element Analysis and Testing of Commercial Vehicle Wheels”, Int. J. of 3D Printing Tech. Dig. Ind., 2020, 4(2): 86-96. 10.46519/ij3dptdi.704994
4. Mazzoni A., Solazzi L., “Experimental field test on a multipiece steel wheel and influence of the material properties on its fatigue life evaluation” Engineering Failure Analysis, 2022, Volume 135, 106106, ISSN 1350-6307, 10.1016/j.engfailanal.2022.106106.
5. Kamal M.B., Vinothkumar S., Srinivasan S., Nesarikar A.S., “Simulation and Test Correlation of Wheel Impact Test. Improvement in the Wheel Design Using Realistic Loading Conditions – FEA and Experimental Stress Comparison” Society of Automotive Engineers International, 2011, 10.4271/2011-28-0129.
6. Kamal M.B., Oery T., Sankaran R.T., Nesarikar A.S., “Simulation and Test Correlation of Wheel Radial Fatigue Test” Society of Automotive Engineers International, 2013, 10.4271/2013-01-1198.
7. Dhumal H., Dindore N., Gavali D., Betgeri P., “Design and Analysis of an Automotive Wheel Rim with the Selection of Optimal Material using Weighted-Properties Method”, International Journal for Research in Engineering Application & Management (IJREAM), 2019, 5(2), 106-117.
8. Kumar K., Singh A., Madan A.K., “FEA Analysis of Car Rim” International Research Journal of Engineering and Technology (IRJET), 2023, 10(4), 748-755.
9. Kumbhar R., Pawar S., Jadhav D., Dhanrale N., “Disc Wheel Rim: CAD Modeling and Correlation between FEA and Experimental Analysis”, International Journal of Engineering Research & Technology, 2014, 3(7), 1316-1321.
10. Islam T., Ahnaf S., Mamun M.M., “Lightweight Design and Structural Analysis of a Wheel Rim Using Finite Element Method and Its Effect on Fuel Economy and Carbon Dioxide Emission”, International Journal of Sustainable Transportation Technology, 2023, 6. 12. 10.31427/IJSTT.2023.6.1.3.
11. EUWA, 2023, ES 3.11 Test requirements for truck steel wheels. Association of European Wheel Manufacturers.

Acknowledgement

We would like to thank Jantsa Wheel Industry and the Graduate School of Natural and Applied Sciences, Department of Mechanical Engineering at Aydın Adnan Menderes University for their valuable contributions to this study.



Licensed under [Creative Commons Attribution-ShareAlike 4.0 International License](https://creativecommons.org/licenses/by-sa/4.0/)